Hindawi
Advances in Civil Engineering
Volume 2021, Article ID 8879900, 13 pages
https://doi.org/10.1155/2021/8879900

Research Article

Study on the Rut Control Threshold of Asphalt Pavement Considering Steering Stability of Autonomous Vehicles Based on Fuzzy Control Theory

Binshuang Zheng,[1] Xiaoming Huang ,[1] Runmin Zhao,[1] Zhengqiang Hong,[1] Jiaying Chen,[1] and Shengze Zhu[1,2]

[1]*School of Transportation, Southeast University, Nanjing 210096, China*
[2]*Shanghai Jiushi (Group) Co., Ltd., Shanghai 200021, China*

Correspondence should be addressed to Xiaoming Huang; huangxm@seu.edu.cn

Received 8 May 2020; Revised 15 February 2021; Accepted 24 March 2021; Published 17 April 2021

Academic Editor: Abdul Aziz bin Abdul Samad

To fully consider the impact of asphalt pavement rut on steering stability of autonomous vehicles, the sensitivity of various indicators of rut shape to vehicle stability was comprehensively measured, and pavement rut control standards based on comfort demands of autonomous vehicles were investigated. Firstly, a steering control system for autonomous vehicles was built in Simulink according to fuzzy control theory. Then, through orthogonal experiment design theory, different rut shape indicators are simulated in CarSim. The influence sensitivity of different rut shape indicators and the allowable rut range considering driving comfort were studied. The results show that both the rut depth and the rut side angle have a greater effect on the vehicle vertical acceleration within a certain parameter range. The maximum roll angle of vehicle body is mainly affected by the rut depth, and the rut width has a small effect on the vehicle driving stability. Meanwhile, considering human comfort, the rut side angle should not be greater than 1° when the rut depth reaches 2 cm. For autonomous driving, the rut depth should not exceed 2.5 cm. When the rut depth exceeds 2.5 cm, the vehicle body roll angle caused by the rut exceeds the inertial centrifugal force of the vehicle itself, which has a significant impact on the passenger comfort and safety.

1. Introduction

At present, asphalt pavement is adopted over 80% of all kinds of roads built in the world [1]. Compared with cement concrete pavement, asphalt pavement has better skid resistance, higher vehicle ride comfort, higher pavement evenness, and better driving stability. However, it also has the disadvantages of low modulus and it is easy to deform. Due to the characteristics of asphalt mixture, external temperature, and overload of vehicles, the asphalt pavement is prone to produce ruts [2–4]. The typical rut distress of asphalt pavement is shown in Figure 1.

With the rapid development of driverless technology around the world, the unmanned driving of vehicles has also put forward higher requirements for road engineering. As the direct carrier of autonomous vehicles, the condition of road surface is undoubtedly the most important and direct impact on the driving safety. The existence of ruts will not only affect the driving comfort, but also the lateral stability and safety of the vehicle when it runs on the road. At present, the main type of the base of asphalt pavement in China is semirigid base, and the rut caused by the shear failure of pavement structure is fairly common. With the bump and pothole on the road surface, the rut makes it easy for water to gather and cause hydroplaning, which increases its influence on driving comfort, stability, and safety. Therefore, it is of great significance for the driving safety and applicability of autonomous vehicles to propose the corresponding rut threshold control standards.

A large number of experiments and practical investigations have been made on asphalt pavement rut [5–7]. It

Figure 1: Typical rut distress of asphalt pavement.

was initially carried out in the AASHO test roads in 1962 in the United States [8], and the causes of pavement rut were systematically studied and explained firstly. The Shell Group of Companies also proposed the design method of asphalt pavement considering rut effect. In Hofstra's report, according to the AASHO's results, the main reason for rutting of asphalt pavement is the lack of shear resistance of pavement materials. Moreover, according to the data of AASHO test road, the rut depth of asphalt pavement is positively correlated with the thickness of asphalt pavement, but when the thickness of asphalt surface layer increases to a certain extent, the rut depth will gradually become stable. Many scholars used numerical simulation, specification, and empirical evaluation methods [9–12] for the research on rut control of asphalt pavement. Based on the tire-pavement interaction model, Ong and Fwa [13–15] carried out quantitative analysis of rut threshold. A rutting prediction procedure was proposed with the theological model and viscoelastic theory. Combining with field test, the parameters related to rutting prediction were determined and a nomograph of rutting calculation was presented [16]. Zhang [17] adopted cylindrical specimen for the test, established the dynamic stability conversion formula between cylindrical specimen and flat specimen, and proposed the calculation method of rut threshold controlling index according to DS (dynamic stability). Javila [18] proposed the concept of RI (rutting index) and "reinforcement effect" based on the new multistress analysis model. Many researchers also advocate the use of RDI (rutting depth index), IRI (international roughness index), and other indicators as the calculation criteria. Based on Burger's model, a finite element model of temperature and load coupling was established to construct a rutting prediction model with axle load, times of load, and road surface temperature as three factors [19]. According to the dynamic modulus test and standard wheel track rut test of asphalt mixture, a rutting prediction model incorporating factors as asphalt layer thickness, loading number, and dynamic modulus indicator was established [20].

In some developed countries, rut control is stipulated in relevant asphalt pavement specifications [21, 22]. For example, Caltrans stipulates [23] that when the rut depth is greater than 1 inch (25.4 mm), it shall be corrected, while the allowable rut depth is considered as the control method of design speed function in Russia. Gendy [24] conducted a questionnaire on the possible road surface deteriorations in Canada and the United States. The results showed that most experts had the opinion that when the rutting depth was greater than 0.375 inch (9.525 mm), corresponding repair should be carried out. However, in the existing research and specifications, only the rut depth is considered as the control index, and other indexes such as rut shape that affect the vehicle stability are not considered. In the current specification in China, 15 mm is adopted as the critical depth of rut without distinguishing road sections and vehicle speed, which may cause certain danger, reducing of the efficiency of rut maintenance and repair, and increasing of the cost.

From the aspect of the vehicle, most of the researchers used CarSim to simulate the driving stability of vehicles [25]. For example, Guo et al. [21] established a straight road model by using CarSim and input different adhesion coefficients to simulate the wheel stress under different rut depth filled with water and mainly analyzed the lateral stability under different speeds. Shahab and Mahyar [26] designed a coordination strategy based on fuzzy logic to coordinate each subcontrol. The vehicle sideslip angle and yaw rate were regarded as the criteria of lateral stability. Wang et al. [27] also established a 3-DOF nonlinear dynamic model with MATLAB/Simulink and proposed a method to increase the roll steering coefficient appropriately. Nowadays, on the path to completely autonomous vehicles, safety, stability, and comfort are the ultimate goal. Therefore, the proposed control architecture can automatically and accurately track the desired trajectory at a set speed while ensuring the stability and riding comfort of autonomous vehicles [28, 29]. Especially, on rutting road, it should be focused on importantly. Recently, some researchers have devoted to investigate the lateral motion based on fuzzy control theory [30, 31] and the lateral control methods of autonomous vehicles considering the asphalt pavement performance. For example, an intelligent fuzzy steering control strategy is proposed to simulate human decision making and analogical reasoning [32, 33]. Furthermore, an optimal control formulation was also developed to obtain the optimal braking and steering patterns in autonomous safety-critical manoeuvres by Fors et al. [34]. From the aspect of pavement rut performance, Ordonez proposed a laser-based rut detection and tracking algorithm to improve the safety and lateral stability of autonomous vehicles considering the benefits of rut following [35, 36]. To reduce

the development rate of rut depth and material fatigue, Chen proposed appropriate lateral control mode with the lateral distribution of autonomous trucks [37]. However, the current research studies always neglect the effect of rut pavement condition on the lateral stability of autonomous vehicles [38–40]. As well as known, the road surface condition, such as rut forms and water film thickness in rut groove, can directly influence the tire-road surface interaction and furtherly affect the lateral stability and ride comfort of autonomous vehicles during steering process.

In view of above research shortcomings, in order to provide reference for the control standard of ruts in the future engineering application, the influence of different rut indexes on driving stability and comfort of autonomous vehicles was investigated in this study. Then, rut threshold of asphalt pavement under different evaluation indexes of autonomous vehicle stability was put forward. We firstly established the steering control system based on the fuzzy control theory and then established the vehicle-road coupling models for different rut conditions in CarSim. Afterwards, the significance analysis of rut shape evaluation indexes was carried out by using orthogonal test design.

2. Research Objective

Based on the driving characteristics and human comfort demands of autonomous vehicles, this paper studies the threshold of asphalt pavement rut control for autonomous vehicles. In this study, we focus on the steering control behavior of autonomous vehicles built by CarSim/Simulink co-simulation. With considering vehicle steering stability and road surface rut shape, rut control threshold for different rut shape evaluation indexes was put forward according to orthogonal experimental design theory. The objectives and main contributions of this study are as follows:

(i) In CarSim, the typical A-class hatchback car model is selected as the vehicle body parameter simulated. To reflect the real rutting shape on road surface, rutting shape after geometric trapezoid regularization is defined in the uneven information of road cross section in CarSim.

(ii) A steering control system for autonomous vehicles was built in Simulink according to fuzzy control theory, which can simulate the steering behavior by cosimulation of CarSim and Simulink. Limit steering rate and planning path are obtained to study the lane change process of autonomous vehicle. In Simulink, a triangular membership function is used in fuzzy control. Through the 7 fuzzy control subsets and 35 fuzzy control rules, the autonomous vehicle during the lane change process is realized.

(iii) The orthogonal experimental design theory is applied to simulate the steering stability of autonomous vehicle by CarSim and Simulink cosimulation, rut threshold for different vehicle stability indexes is obtained. As far as we know, this is one of the first attempts in the self-driving area to evaluate steering stability considering road surface rut shape. In our opinion, this approach is of big significance to improve brake safety and comfort of autonomous vehicles.

3. Integrated Vehicle-Road Modeling in CarSim

3.1. Vehicle Model Parameters. Many kinds of vehicle models are preset in the CarSim database, including sedans, SUVs, and vans. According to relevant research [41], since 1984 when the Chinese government liberalized the purchase market of private passenger vehicles, the number of private passenger vehicles in China has increased dramatically. According to the data of China Passenger Car Association (CPCA), China's passenger car ownership at present is mainly composed of Class A0 and Class A cars, and the number of these two classes exceeds 70% of China's total number of passenger cars [42, 43]. Meanwhile, the safety and comfort of Class A cars are far behind other classes, which means that Class A cars are more sensitive to road conditions. Therefore, considering the representativeness and vehicle comfort and safety, Class A model in the CarSim database is selected as the modeling object to ensure that the research results meet the driving needs of the majority of vehicles.

We adopted the "Class A, Hatchback" model in the CarSim database, as shown in Figure 2. The main size data are as follows: the wheelbase is 2347 mm; the distance from the mass center to the ground is 540 mm; the distance between the mass center and the front axle is 1103 mm; and the distance between left and right wheels is 1416 mm. Other parameters, such as vehicle suspension system and power system, are preset in the CarSim database.

3.2. Rut Pavement Model. This paper aims to fully study the sensitivity of different indicators of rut shape on the driving stability of vehicles. In fact, the cross section of asphalt pavement with rut is usually an asymmetrical irregular shape formed by curves. Therefore, it is difficult to directly describe the actual rut shape with multiple indexes, so it is necessary to first geometric regularize the cross section to simplify it to trapezoid, as shown in Figure 3(a). The black line is the actual rut cross section, and the red line is the regularized trapezoid of rut. In this study, the selected indexes of rut shape include rut depth h, side angle α, and rut average width w, and specific definitions of the three indicators are shown in Figure 3(b):

(1) The elevation difference from the bottom of the rut to the highest point of the two shoulders is defined as h

(2) The average inclination angle of the side of the rut is defined as α

(3) The width at half of the rut depth is defined as w

The rut shape is defined in the "irregularity information" of the cross section in CarSim, in which the cross-section coordinates are equally divided at every 0.2 m along the width direction of the pavement with the pavement surface elevation recorded similarly. Meanwhile, to eliminate the

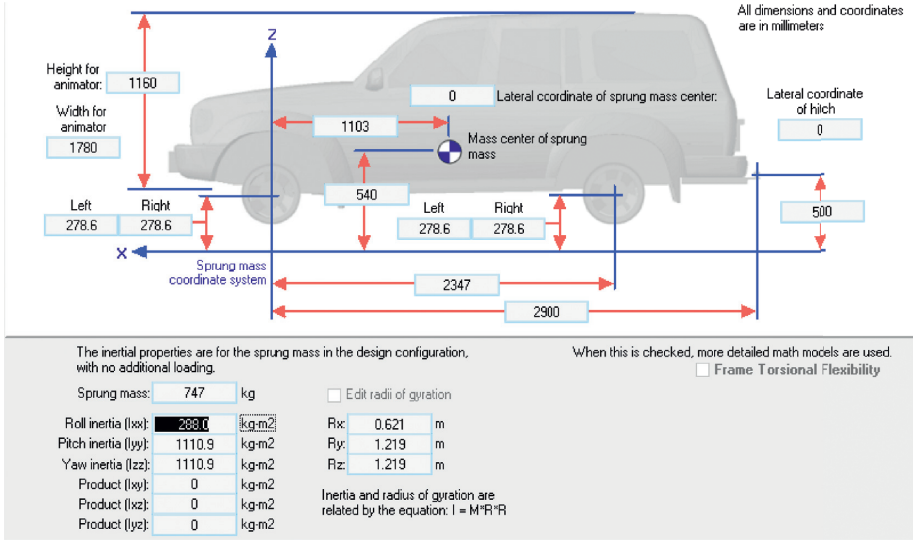

Figure 2: The data of A-class hatchback car in CarSim.

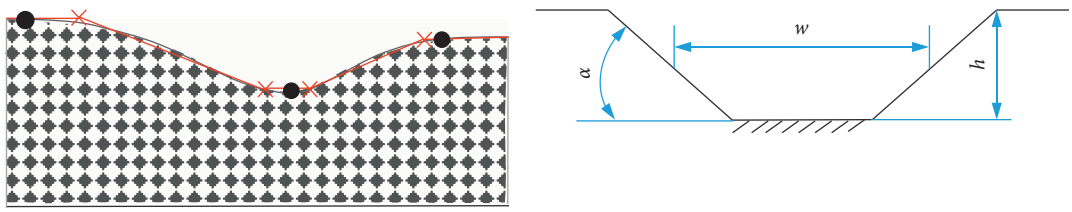

(a) (b)

Figure 3: Architecture of rut shape of asphalt pavement. (a) Rut cross section. (b) Rut shape index.

sharp points of ruts after geometric regularization, further coordinate encryption is carried out on the basis of the original 0.2 m equidistant coordinate point. As this study mainly measures the influence of different rut shape indicators on the lateral stability of vehicles, the longitudinal change of rut shape is not considered [44]. The rut parameter setting in CarSim is shown in Figure 4, wherein the horizontal axis refers to the direction along the road, and the vertical axis represents the horizontal direction of the road. In addition, the different colored lines are the horizontal elevation of the road.

4. Steering Control System of Autonomous Vehicles

4.1. Lane Change Subsystem Based on Fuzzy Control Theory. Generally, during the normal lane change of the vehicle, the steering angle of the front wheel is the smallest, and the maximum steering angle is usually stable around 15°. Under the conditions of the vehicle turning around, it is usually necessary to take the limit steering angle of the vehicle front wheel, that is, about 40°. And during the turning process, the front wheel angle is usually between 15° and 40°. At present, in the steering control system of an autonomous vehicle, the above three different steering conditions are usually separated and controlled separately by different subsystems. At the same time, through a unified control center, the steering conditions required for autonomous vehicles are distinguished, and different subsystems are activated to control the steering process of the autonomous vehicles under different driving conditions. The Simulink toolbox in MATLAB was applied to compile the subsystem of lane change for autonomous vehicles. Furtherly, the Simulink control system was connected to the CarSim simulation interface to carry out the simulation of the lane change process of the autonomous vehicle to fully measure the influence of different rut patterns on the vehicle stability and driving comfort under the condition of autonomous driving.

In the lane change subsystem, the angle β of vehicle deviation is defined as the difference between the planned heading angle of an autonomous vehicle and the actual heading angle of the current vehicle, that is $\beta = b - a$. Lateral deviation S is defined as the vertical distance between the center of gravity of unmanned vehicle and the planned theoretical vehicle route. The fuzzy control system is divided into seven fuzzy control subsets. These seven fuzzy control subsets are used to define the vehicle deviation angle β and the vehicle front wheel output rotation angle u. Five fuzzy control subsets of NB, NS, ZE, PS, and PB are chosen to define the vehicle lateral deviation S. Thus, 35 fuzzy control rules are formulated:

(1) If S is NB and β is NB, then u is NM

(2) If S is NB and β is NM, then u is NS

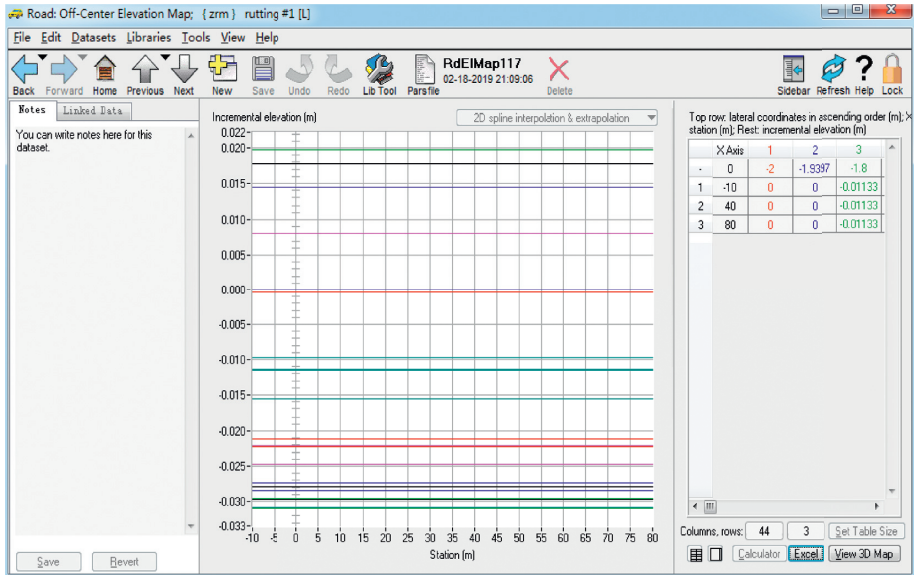

Figure 4: Pavement rut parameter setting in CarSim.

(3) If S is NB and β is NS, then u is NS
(4) If S is NB and β is ZE, then u is PS
(5) If S is NB and β is PS, then u is PS
(6) If S is NB and β is PM, then u is PM
(7) If S is NB and β is PB, then u is PB
(8) If S is NS and β is NB, then u is NM
(9) If S is NS and β is NM, then u is NM
(10) If S is NS and β is NS, then u is NS
(11) If S is NS and β is ZE, then u is ZE
(12) If S is NS and β is PS, then u is PS
(13) If S is NS and β is PM, then u is PM
(14) If S is NS and β is PB, then u is PM
(15) If S is ZE and β is NB, then u is NB
(16) If S is ZE and β is NM, then u is NM
(17) If S is ZE and β is NS, then u is NS
(18) If S is ZE and β is ZE, then u is ZE
(19) If S is ZE and β is PS, then u is PS
(20) If S is ZE and β is PM, then u is PM
(21) If S is ZE and β is PB, then u is PB
(22) If S is PS and β is NB, then u is NM
(23) If S is PS and β is NM, then u is NS
(24) If S is PS and β is NS, then u is NS
(25) If S is PS and β is ZE, then u is ZE
(26) If S is PS and β is PS, then u is PS
(27) If S is PS and β is PM, then u is PS
(28) If S is PS and β is PB, then u is PM
(29) If S is PB and β is NB, then u is NB
(30) If S is PB and β is NM, then u is NM
(31) If S is PB and β is NS, then u is NS
(32) If S is PB and β is ZE, then u is NS
(33) If S is PB and β is PS, then u is PS
(34) If S is PB and β is PM, then u is PS
(35) If S is PB and β is PB, then u is PM

The fuzzy domain for the input and output variables is defined as $[-3, 3]$. As for the three different variables, their actual physics domains are different. For the actual physics domain, the lateral deviation S of vehicle is $[-1, 1]$, the angle β of vehicle deviation is $[-25, 25]$, and the output angle u of vehicle steering wheel takes $[-30, 30]$. Thus, through calculation, we can see that the corresponding domain conversion scale factors of the three variables are as follows: $KS = 3/1 = 3$ (physics domain is transformed into fuzzy domain); $K\beta = 3/25 = 0.12$ (physics domain is transformed into fuzzy domain); $Ku = 30/3 = 10$ (fuzzy domain is transformed into physics domain).

Regarding the determination of the membership function, the definition of two input variables S and β and one output variable u is carried out by using the common continuity triangular membership function in current fuzzy control systems. The membership functions of the three parameters are shown in Figure 5.

In this study, it is assumed that there is a virtual steering wheel in the autonomous vehicle. In the Simulink program, the steering angle of the wheel will be converted into the steering wheel rotation angle by a simple fixed expansion factor. Thus, by controlling the rotation angle of the virtual steering wheel, the steering angle of the front wheels is controlled indirectly. Among them, the relationship between the angle of the steering wheel and the lateral displacement of the steering lever is shown in Figure 6(a), and the relationship between the lateral displacement of the steering lever and the steering angle of the right front wheel is shown in Figure 6(b).

From Figure 6, when the steering angle of the inner wheel changes from 0° to 51.8207°, the ratio of the steering wheel angle to the inner wheel angle changes from 13.70183

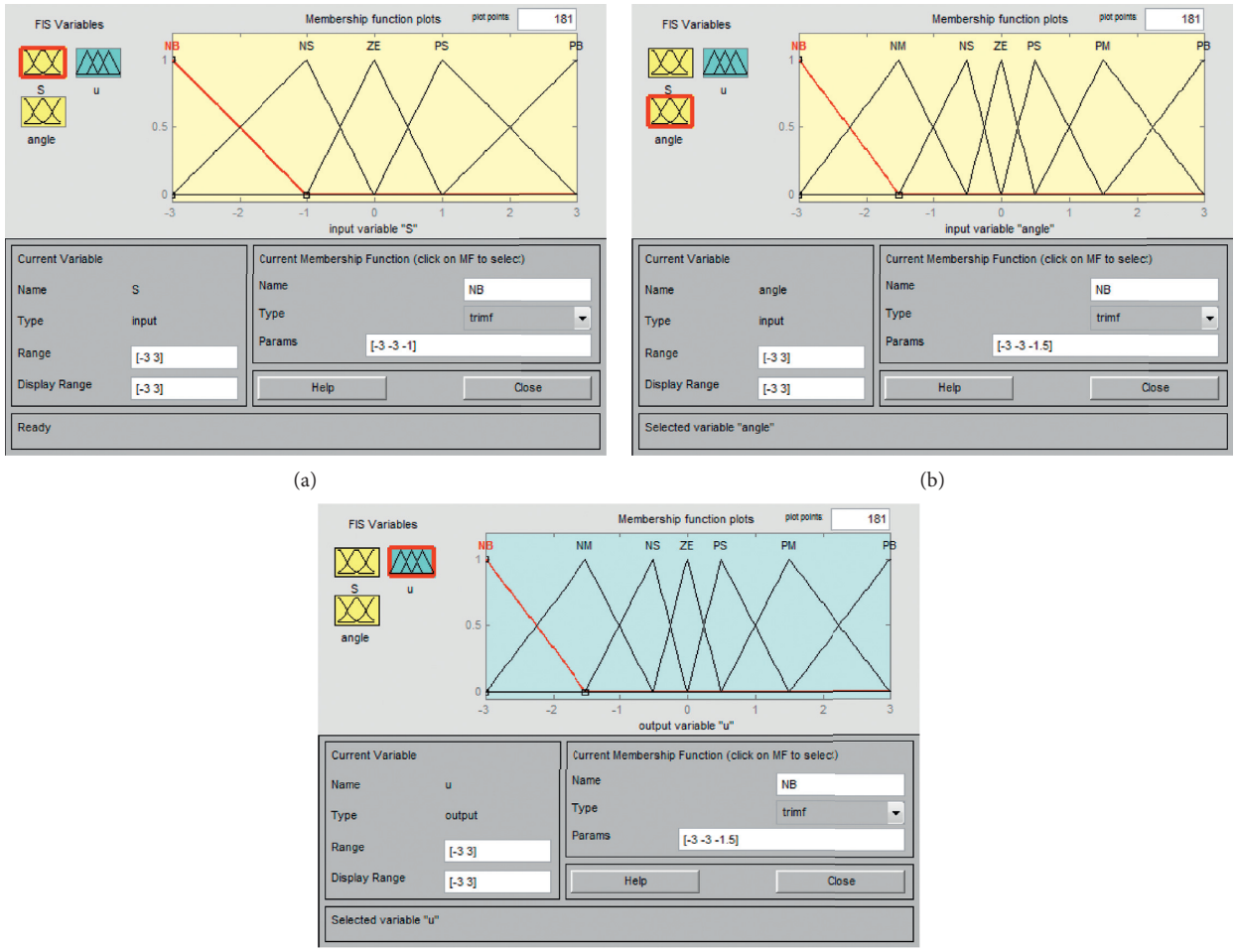

Figure 5: Membership functions of parameters. (a) Input parameter, S. (b) Input parameter, β. (c) Output parameter, u.

to 14.93546. Moreover, as the steering angle increases, the ratio also tends to increase monotonously. In order to simplify the model, the ratio is taken as the average of different data points, which is 14.5. Thus, in Simulink control program, the wheel angle in the fuzzy control system is multiplied by the steering wheel angle expansion factor to control the steering wheel angle of the autonomous vehicles in CarSim.

4.2. Lane Change Path and Limit Steering Rate Design. In the path processing and lane changing system module in Simulink, the current location of the unmanned vehicle is located, so as to determine the corresponding line coordinate matrix data line for calculation control and output of the wheel steering angle. The coordinate matrix of path planning is [A*4] matrix, among which, A represents the number of path segments. Each row in the matrix represents a path segment, and each row has two coordinate points and four data, respectively, representing the starting point coordinate value X_1 and Y_1 and end point coordinate value X_2 and Y_2 of the path segment, as shown in Figure 7.

When the distance between the center of the vehicle mass and the end point coordinates X_2 and Y_2 of the current path segment is less than 1.0, which is determined to pass the current path segment. The route processing and lane change system judges to enter the next route segment and controls the steering angle of the autonomous vehicle according to the starting point and end point coordinate values of the next route segment and the driving path angle. Regarding the conditional control that the car body cannot invade the third lane during the lane change process, the vehicle body width is taken to be 2 m for conservative control.

In order to ensure that the vehicle does not interfere with the operation of the vehicle in the third lane during the lane change process, the offset of the vehicle body centerline should not be greater than 5 m. The specific control program in Simulink is shown in Figures 8 and 9.

In the steering rate control process, this study uses the ratio to describe, that is, the ratio of the distance traveled by the vehicle in the driving direction to the vehicle lateral offset distance. In order to determine the limit steering rate under different vehicle speeds in the case of the automatic fuzzy control system, ased by steps of 5 m, and the lateral

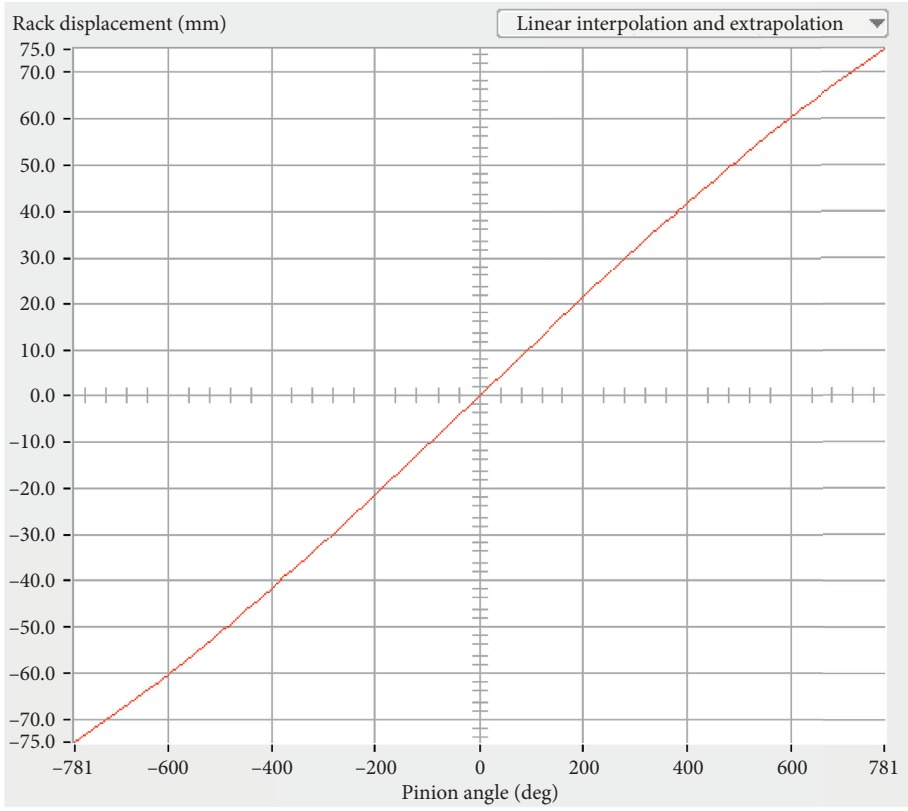

Figure 6: Relationship between steering angle and lateral displacement of steering lever during steering process. (a) Angle of steering wheel-lateral displacement of steering lever. (b) Lateral displacement of steering lever-steering angle of rear wheel.

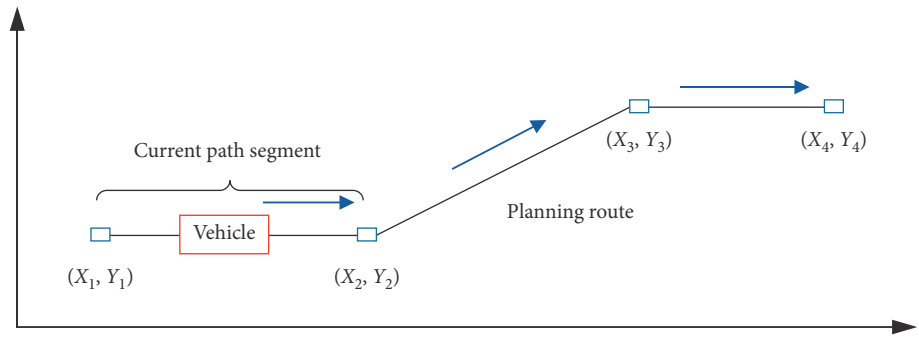

Figure 7: Architecture of the path matrix.

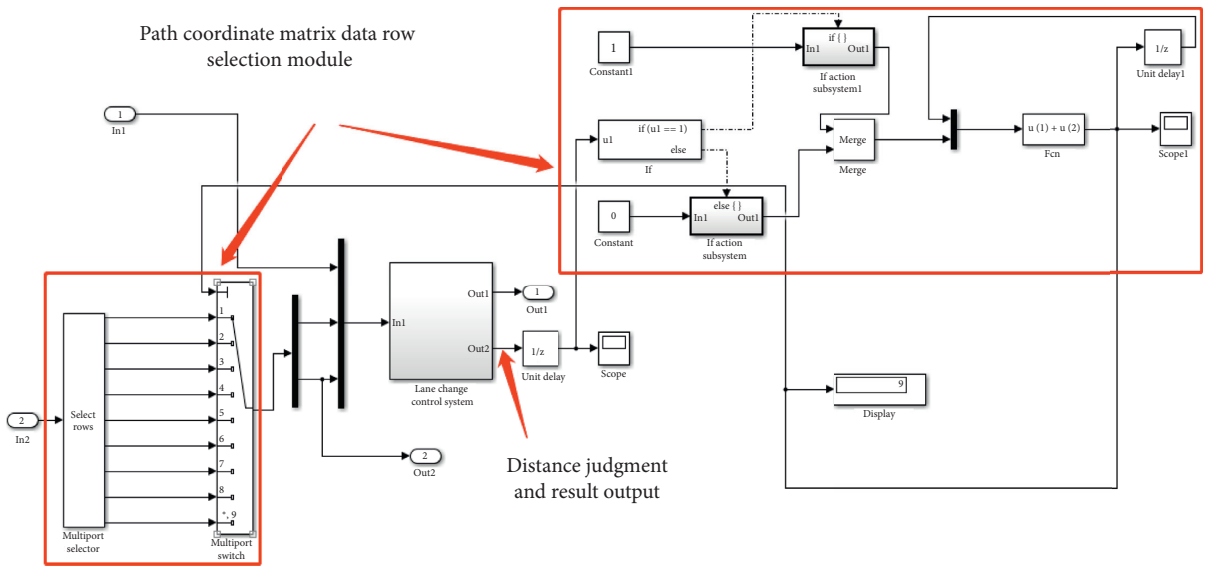

Figure 8: Path handling and lane change subsystem.

displacement of the vehicle after the lane change is 4 m. Each running speed corresponds to two adjacent lane change rates to determine the final limit lane change rate of autonomous vehicle at different speeds. In order to ensure that the vehicle body can be kept within the design path, the maximum steering rate simulated at different speeds, as shown in Figure 10.

At the speed of 120 km/h, setting the steering rate as 50 : 4 during normal driving process, the vehicle can reach the limit state where the body does not invade the third lane during operation. The maximum offset of the vehicle is close to 5 m, but the vehicle body remains in the preset lane. In the following simulation of rut threshold, the limit steering rate was adopted at the speed of 120 km/h, and the coordinate matrix of planning path (L (120)) is as follows:

$$[L(120)] = \begin{bmatrix} 0 & 0 & 100 & 0 \\ 100 & 0 & 150 & 4 \\ 150 & 4 & 180 & 4 \\ 180 & 4 & 200 & 4 \\ 200 & 4 & 300 & 4 \\ 300 & 4 & 400 & 4 \\ 400 & 4 & 500 & 4 \\ 500 & 4 & 600 & 4 \\ 600 & 4 & 700 & 4 \end{bmatrix}. \quad (1)$$

5. Vehicle Steering Stability Simulation in CarSim

The influence of road rutting on vehicle driving stability is mainly reflected in the two indexes of the vehicle vertical acceleration and vehicle body roll angle. The passenger comfort mainly depends on the change of speed, that is, vehicle vertical acceleration. Meanwhile, the ISO 2631–1 [45] promulgated by the International Organization for Standardization also gives the comfort level of human body for different accelerations. Therefore, the two indexes of vehicle roll angle and vertical acceleration were selected in this study.

5.1. Identification of Limit Friction Coefficient. As the vehicle speed is large while the friction between tire and road surface is low, the vehicle will have a serious uncontrollable phenomenon during the steering process. In CarSim, set the vehicle speed of 120 km/h with steering rate of 25 : 1. With the friction coefficient of 0.1, the steering control process is conducted by the fuzzy control system for autonomous vehicles built in Simulink, and vehicle body coordinate point during lane change is as shown in Figure 11.

During the process of vehicle change lane, the steering force provided by small road friction is too low, and the vehicle cannot achieve sufficient self-aligning torque. As a result, the vehicle cannot be controlled in the target lane in time, causing the body to invade the outer lane seriously, which seriously affects the safety of the vehicle when changing lanes. According to adjust the friction coefficient properly, as the friction coefficient is 0.14 at the speed of 120 km/h, the vehicle can reach the limit state where the body does not invade the third lane during operation, as shown in Figure 12.

5.2. Simulation Results Based on Orthogonal Experimental Design. In order to study the influence degree of different rut shape indexes on vehicle stability during steering process, the combination design of different rut shape indexes was carried out by orthogonal experimental design theory in CarSim simulation. Three influence factors including rut depth, average rut width, and rut lateral angle are considered in the study. Thus, the L-9-3-4 orthogonal design table was selected for the combined design scheme, and set three levels for each factor. Then, the design scheme for the CarSim simulation is shown in Table 1.

For rut mainly affects the lateral unevenness of the road surface, lateral lane change behavior is added in the simulation,

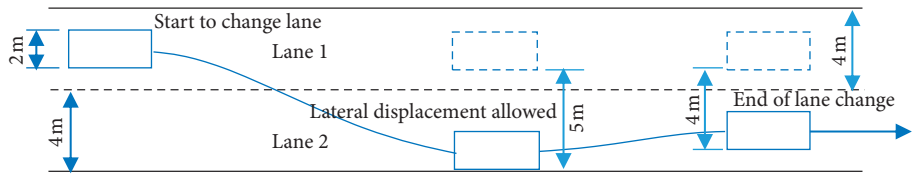

Figure 9: Architecture of vehicle distance during lane change.

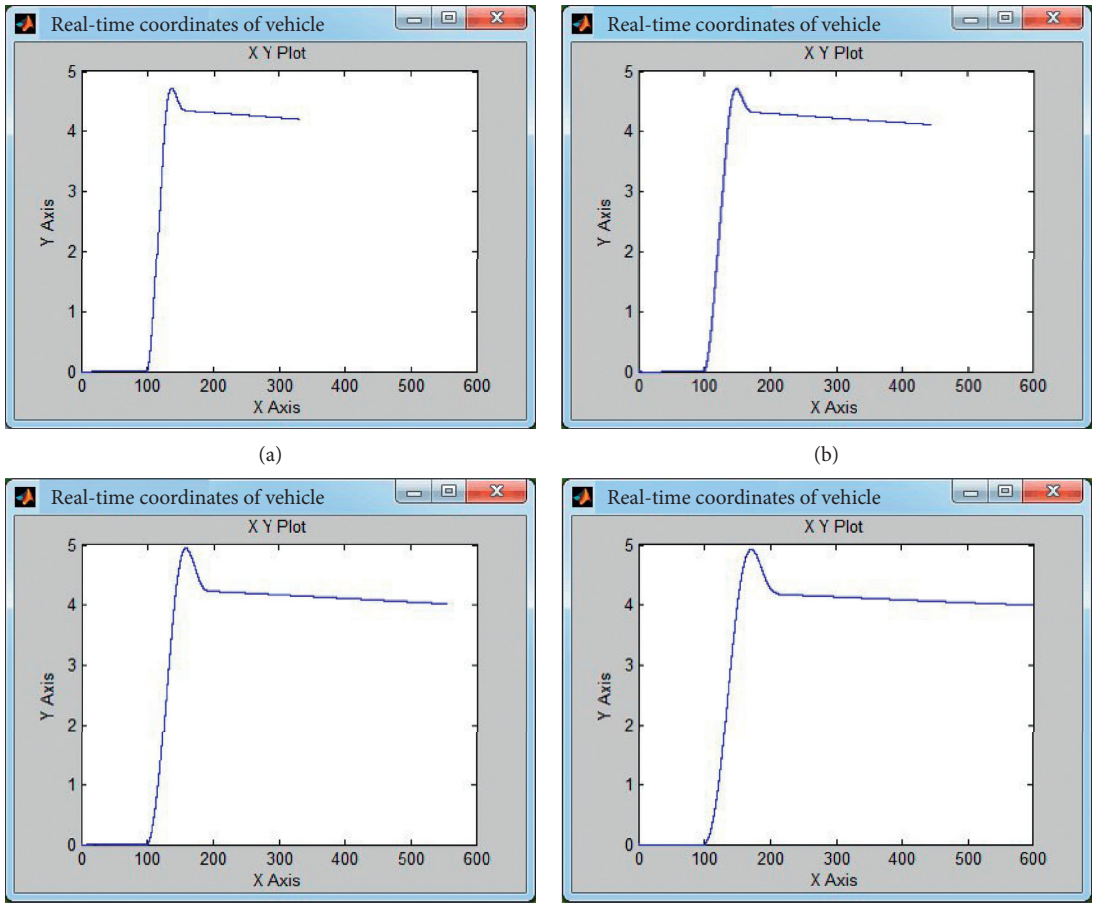

Figure 10: Limit steering rate design for different speeds. (a) Steering rate of 25 : 4 with a speed of 60 km/h. (b) Steering rate of 35 : 4 with a speed of 80 km/h. (c) Steering rate of 40 : 4 with a speed of 100 km/h. (d) Steering rate of 50 : 4 with a speed of 120 km/h.

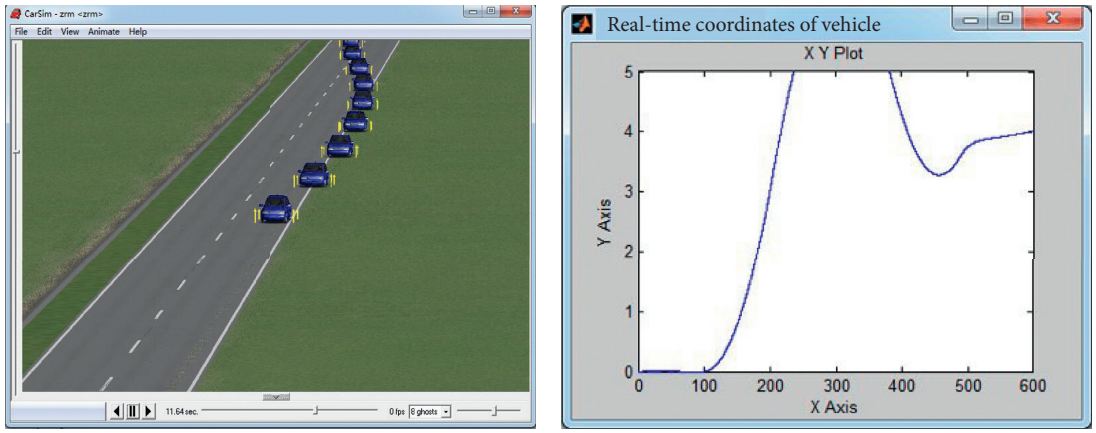

Figure 11: Simulation with a vehicle speed of 120 km/h and friction coefficient 0.10. (a) The simulation interface in CarSim. (b) The vehicle lateral displacement plot.

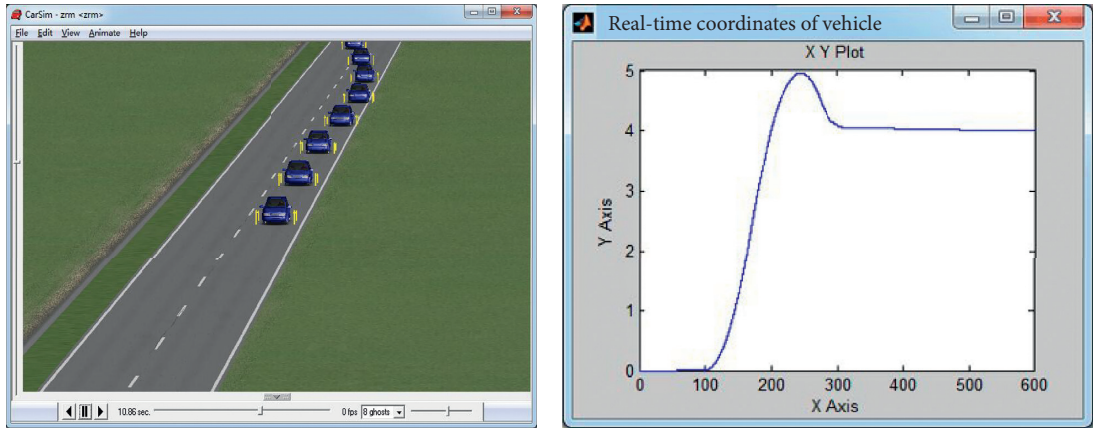

(a) (b)

Figure 12: Simulation with a vehicle speed of 120 km/h and friction coefficient 0.14. (a) The simulation interface in CarSim. (b) The vehicle lateral displacement plot.

Table 1: Results of orthogonal experimental design.

Test number	1	2	3	4	5	6	7	8	9
h (cm)	1	1	1	1.5	1.5	1.5	2	2	2
α (°)	1	2	3	1	2	3	1	2	3
w (cm)	80	100	120	100	120	80	120	80	100

so that the vehicle crosses the uneven section. Considering the most unfavorable situation, the limit speed of the highway is 120 km/h as the simulated speed, and the steering rate of the vehicle is 25 : 1 with road surface friction coefficient of 0.14.

In the simulation process, the vehicle vertical acceleration and roll angle are not only caused by rutting, but also the inertial centrifugal force of vehicle and suspension system performance. Therefore, in order to avoid the inertial effect of the vehicle during the steering process, it is necessary to deduct the simulation results of the vehicle on a completely flat road under the same working conditions. The simulation interface and the lateral displacement of the vehicle are obtained as shown in Figure 11, which is completely caused by rutting. The simulation results of vehicle vertical acceleration and roll angle are shown in Table 2.

5.3. Sensitivity Analysis of Rut Shape Evaluation Indexes. According to Table 2, the range analysis of the maximum vertical acceleration and roll angle of the vehicle body is carried out, as shown in Table 3 and Table 4. It can be seen that the range of the rut depth is the largest for the maximum vertical acceleration of the vehicle; that is, the effect of the rut depth on the maximum vertical acceleration is the most significant, followed by the slide angle of the rut in Table 3. And the range of the rut average width is the smallest. Therefore, compared with the effects of rut depth and rut side angle, the effect of the rut average width on the maximum vertical acceleration of the vehicle can be negligible.

From Table 4, it can be seen that the range of rut depth is still largest, while the range values for both the rut side angle and the rut average width are 3 times smaller than the rut depth. Therefore, the influence of rut depth on the maximum roll angle of the vehicle body is the most significant, while the influence of the rut side angle and the average width of the rut can be neglected.

6. Rut Threshold under Different Evaluation Indexes

6.1. Vehicle Body Roll Angle. Selecting the maximum roll angle of the autonomous vehicle as the control index, only the rut depth needs to be considered. The allowable threshold was calibrated for the maximum rut depth. In the study, the rut depth was set as 1 cm, 1.5 cm, 2 cm, 2.5 cm, and 3 cm, respectively. When the vehicle drives on a completely straight road under the same condition, the maximum roll angle during the lane change process is 1.1063610°. The maximum roll angle of the autonomous vehicle caused by rut is shown in Figure 13.

Based on the principle that the maximum roll angle of the vehicle body caused by rutting should not exceed the maximum roll angle of the vehicle during the lane change process, the rut depth under unmanned driving conditions should not exceed 2.5 cm. When the rut depth exceeds 2.5 cm, the vehicle body roll angle caused by the rut exceeds the inertial centrifugal force of the vehicle itself, which has a significant impact on the passenger comfort.

6.2. Vehicle Vertical Acceleration. For further simulation of the maximum vertical acceleration of the vehicle, rut depth and rut side angle were selected as variables. When the rut side angle is set as 1°, the rut depth cannot reach 2.5 cm and deeper depth under the normal rut width range. However, when the rut side angle changes from 2° to 3°, the rut depth

Table 2: Simulation results of the orthogonal experiment design.

Test no.	Rut depth H (cm)	Rut slide angle α (°)	Average rut width B (cm)	Maximum vertical acceleration (g's)	Vehicle roll angle (deg)
1	1.0	1	80	0.01668	0.026954
2	1.0	2	100	0.02207	0.022685
3	1.0	3	120	0.023782	0.019744
4	1.5	1	100	0.017902	0.039066
5	1.5	2	120	0.020326	0.031618
6	1.5	3	80	0.026792	0.037611
7	2.0	1	120	0.025492	0.066289
8	2.0	2	80	0.033325	0.054974
9	2.0	3	100	0.037105	0.046514

Table 3: Analysis results of the vehicle maximum vertical acceleration.

Factors	h (cm)	α (°)	w (cm)
Average value 1	0.021	0.020	0.026
Average value 2	0.022	0.025	0.026
Average value 3	0.032	0.029	0.023
Range	0.011	0.009	0.003

Table 4: Analysis results of the maximum vehicle roll angle.

Factors	h (cm)	α (°)	w (cm)
Average value 1	0.023	0.044	0.040
Average value 2	0.036	0.036	0.036
Average value 3	0.056	0.035	0.039
Range	0.033	0.009	0.004

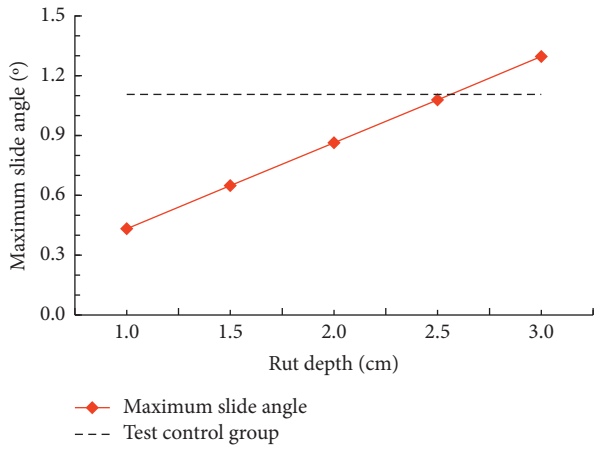

Figure 13: Simulation results of the vehicle maximum roll angle.

Table 5: Comfort zone division based on the standard ISO-2631.

Comfortable			Slightly uncomfortable		
h (cm)	α (deg)	a_{max} (m·s^{-2})	h (cm)	α (deg)	a_{max} (m·s^{-2})
1.0	1	0.163464	2.0	2	0.326634
1.0	2	0.216286	2.0	3	0.363678
1.0	3	0.233044	2.5	2	0.337512
1.5	1	0.17542	2.5	3	0.462756
1.5	2	0.199234	3.0	2	0.321538
1.5	3	0.262542	3.0	3	0.486766
2.0	1	0.249802	—	—	—

can reach 3 cm within the rut width range. Therefore, when the rut depth is greater than or equal to 2.5 cm, the rut side angle is only 2° and 3°. When the rut depth is less than 2.5 cm, there are three rut side angles, such as 1°, 2°, and 3°.

As the rut depth and rut side angle increase, the maximum vertical acceleration of autonomous vehicle will increase significantly. However, the maximum vertical acceleration of the vehicle did not exceed 0.5 m/s^2. According to the standard ISO 2631–1, the passenger comfort level for different acceleration ranges is specified corresponding. The simulation experiment results are distinguished according to the two categories of "comfortable" and "slightly uncomfortable", as shown in Table 5.

The results in Table 5 show that when the rut depth changes from 1 cm to 2.5 cm and the rut side angle changes from 1° to 3°, the maximum vertical acceleration of the unmanned vehicle body will exceed the acceleration range of "keep comfortable" specified in ISO-2361, then belongs to the state of "slightly uncomfortable". The specific results are as follows:

(1) When the rut depth is 1.5 cm or less, regardless of the rut side angle value (not more than 30°), the vehicle vertical acceleration can be kept within the "keep comfortable" range.

(2) When the rut depth is increased to 2 cm, only the rut side angle is less than or equal to 1°, the vertical acceleration of the vehicle can be kept within the "keep comfortable" state. If the rut depth or rut side angle continues to increase, passenger will feel "slightly uncomfortable."

(3) As the rut side angle reaches 3° and the rut depth reaches 2.5 cm or 3 cm, the maximum vertical acceleration of the vehicle during the lane change process will be close to 0.5 m/s^2, and the passenger comfort will be significantly affected.

According to the above analysis, for the maximum vertical acceleration of autonomous vehicles, the rut depth should generally not be greater than 1.5 cm considering the passenger comfort. Moreover, when the rut depth reaches 2 cm, the rut side angle should not be greater than 1°.

7. Conclusions

Based on the cosimulation of CarSim and Simulink, the fuzzy control theory is used to build the steering control

system of autonomous vehicles. The orthogonal experimental design theory was adopted to combine different rut shape indexes. And the driving stability of autonomous vehicles on the rut road during the lane change process was simulated in CarSim. Reference to the allowable rut range of passenger comfort, rut control threshold of asphalt pavement was studied. The main research conclusions are as follows:

(1) Rutting has a significant effect on the stability of the autonomous vehicle. When considering the maximum vertical acceleration of the car body during the lateral crossing of the rut, the rut depth and the rut side angle both have significant impact, while the rut width influence can be ignored. For the roll angle of the vehicle, only the influence of rut depth needs to be considered.

(2) Considering the influence of pavement rut, the rut depth should generally not be greater than 1.5 cm to ensure the passenger comfort. Moreover, when the rut depth reaches 2 cm, the rut side angle should not be greater than 1°. Under unmanned driving condition, the rut depth should not exceed 2.5 cm. When the rut depth exceeds 2.5 cm, the vehicle body roll angle caused by the rut exceeds the inertial centrifugal force of the vehicle itself, which has a significant impact on the passenger comfort.

(3) In the rut threshold control standard, because the influence of rut width on the maximum roll angle and the maximum vertical acceleration of the vehicle body is small in the simulation analysis of the orthogonal test, the rut width may not be regarded as the control standard.

Due to the lack of relevant evaluation standards for human comfort for the roll angle of vehicle, this study does not give the rut control threshold recommendations for the roll angle as an evaluation index. Furtherly, this work still needs to be studied combing with the field test.

Data Availability

The simulation data used to support the findings of this study are included within the article.

Additional Points

Summary. In this study, the influence law of different rut indexes on driving stability and comfort of autonomous vehicles is studied. Then, rut threshold of asphalt pavement under different evaluation indexes of autonomous vehicle stability was put forward. This study can provide reference for the control standard of ruts in the future engineering application.

Conflicts of Interest

The authors declare that they have no conflicts of interest regarding the publication of this paper.

Acknowledgments

The study was financially supported by the National Natural Science Foundation of China (no. 51778139).

References

[1] X. Song, "Discussion on application and development of asphalt pavement," *Architecture Technology and Management*, vol. 13, pp. 30-31, 2017.

[2] Y. Jia, "Discussion on rutting problem of asphalt pavement," *Construction & Design for Project*, vol. 20, pp. 64-65, 2019.

[3] R. Behnke, I. Wollny, F. Hartung, and M. Kaliske, "Thermo-mechanical finite element prediction of the structural long-term response of asphalt pavements subjected to periodic traffic load: tire-pavement interaction and rutting," *Computers & Structures*, vol. 218, pp. 9–31, 2019.

[4] N. Hossain, D. Singh, M. Zaman, and D. H. Timm, "Performance monitoring of field test section to evaluate rutting behavior of different pavement layers," *International Journal of Pavement Research and Technology*, vol. 12, no. 5, pp. 519–526, 2019.

[5] American Association of State Highway and Transportation Officials, *AASHTO Guide for Design of Pavement structures*, American Association of State Highway and Transportation Officials, Washington, DC, 1993.

[6] C. Monismith, R. Hicks, F. Finn et al., *Permanent Deformation Response of Asphalt Aggregate mixes. SHRP-A-415, Strategic Highway Research Program, Transportation Research Board*, National Research Council, Washington, DC, 1994.

[7] A. Simpson, J. Daleiden, and W. O. Hadley, *Rutting Analysis from a Different perspective, Transportation Research Board*, pp. 9–17, National Research Council, Washington, DC., 1995.

[8] H. Titin, *The Frame Work of Statistical Acceptance Plan Based on the Permanent Deformation Potential of Asphalt Concrete*, The Pennsylvania State University, Pennsylvania, USA, 2001.

[9] R. Barksdale, "Laboratory evaluation of rutting in base course materials,"vol. 01, pp. 161–174, in *Proceedings 3rd International Conference on the Structural Design of Asphalt Pavements*, vol. 01, pp. 161–174, International Society for Asphalt Pavements, Lino Lakes, MN, August 1972.

[10] N. Lister and R. Addis, *Field Observations of Rutting and Practical implications*, pp. 28–34, Transportation Research Board, Washington, DC, 1977.

[11] J. Sousa, J. Craus, and C. Monismith, *Summary Report on Permanent Deformation in Asphalt Concrete*, Strategic Highway Research Program (SHRP), Washington, DC, 1991.

[12] S. Xu and Z. Zhu, "Review of rutting prediction methods and control indexes for high-grade roads," *East China Road*, vol. 4, 1991.

[13] G. P. Ong and T. F. Fwa, "Wet-pavement hydroplaning risk and skid resistance: modeling," *Journal of Transportation Engineering*, vol. 133, no. 10, pp. 590–598, 2007.

[14] T. F. Fwa and G. P. Ong, "Wet-pavement hydroplaning risk and skid resistance: analysis," *Journal of Transportation Engineering*, vol. 134, no. 5, pp. 182–190, 2008.

[15] T. F. Fwa, H. R. Pasindu, and G. P. Ong, "Critical rut depth for pavement maintenance based on vehicle skidding and hydroplaning consideration," *Journal of Transportation Engineering*, vol. 138, no. 4, pp. 423–429, 2012.

[16] S. F. Xu and Z. H. Zhu, "Prediction of rutting in asphalt pavement of high-glass road [J]," *Journal of Civil Engineering*, vol. 26, no. 06, pp. 28–36, 1993.

[17] K. Zhang, Z. Zhang, and Y. Luo, "Inspection method and evaluation standard based on cylindrical core sample for rutting resistance of asphalt pavement," *Measurement*, vol. 117, pp. 241–251, 2018.

[18] B. Javilla, L. Mo, F. Hao, B. Shu, and S. Wu, "Multi-stress loading effect on rutting performance of asphalt mixtures based on wheel tracking testing," *Construction and Building Materials*, vol. 148, pp. 1–9, 2017.

[19] W. L. Li, "Research on rutting estimation model of asphalt pavement based on Burgers model," *Highway*, vol. 64, no. 08, pp. 16–22, 2019.

[20] Y. H. Yang, S. L. Zhang, and Q. Zhang, "Rutting depth prediction based on dynamic modulus and three-layer wheel track rutting test," *Journal of Xi'an University of Architecture & Technology*, vol. 51, no. 05, pp. 717–723, 2019.

[21] X. Guo, B. Zhou, and C. Zhang, "Analysis of rutting index for pavement maintenance based on driving safety on surface gathered water consideration," in *Proceedings of the Cota International Conference of Transportation Professionals*, pp. 909–918, Beijing, China, July 2014.

[22] Z. P. Shan, "Rutting formation and allowable depth of asphalt concrete pavement," *Transportation World*, vol. 20, pp. 34-35, 2016.

[23] California dept. Of transportation (Caltrans). Maintenance manual, Volume 1 Caltrans, http://www.dot.ca.gov/hq/maint/manual/maintman.html, 2006.

[24] A. El Gendy, Y. Qi, R. Guo et al., "Survey study of pavement warranty distress thresholds," in *Proceedings of the Second International Conference on Public-Private Partnerships*, Austin, Texas, May 2015.

[25] J. H. Guo and J. Wang, "Lateral stability control of distributed drive electric vehicle based on fuzzy sliding mode control," in *Proceedings of the 2017 IEEE 3rd Information Technology and Mechatronics Engineering Conference*, pp. 675–680, Chongqing, China, October 2017.

[26] R. Shahab and N. Mahyar, "Design of an integrated control system to enhance vehicle roll and lateral dynamics," *Transactions of the Institute of Measurement and Control*, vol. 40, no. 5, pp. 1435–1446, 2018.

[27] G. L. Wang, J. Yang, X. F. Fan et al., "Vehicle steering motion simulation based on MATLAB/Simulink," *Journal of Highway and Transportation Research and Development*, vol. 06, pp. 157–161, 2006.

[28] J. Guo, K. Li, and Y. Luo, "Coordinated control of autonomous four wheel drive electric vehicles for platooning and trajectory tracking using a hierarchical architecture," *Journal of Dynamic Systems, Measurement, and Control*, vol. 137, no. 10, Article ID 101001, 2015.

[29] J. Chen, Z. Shuai, H. Zhang, and W. Zhao, "Path following control of autonomous four-wheel-independent-drive electric vehicles via second-order sliding mode and nonlinear disturbance observer techniques," *IEEE Transactions on Industrial Electronics*, vol. 68, no. 3, pp. 2460–2469, 2021.

[30] J. Guo, P. Hu, L. Li, and R. Wang, "Design of automatic steering controller for trajectory tracking of unmanned vehicles using genetic algorithms," *IEEE Transactions on Vehicular Technology*, vol. 61, no. 7, pp. 2913–2924, 2012.

[31] J. Guo, L. Li, K. Li, and R. Wang, "An adaptive fuzzy-sliding lateral control strategy of automated vehicles based on vision navigation," *Vehicle System Dynamics*, vol. 51, no. 10, pp. 1502–1517, 2013.

[32] E. Kayacan, E. Kayacan, H. Ramon et al., "Towards agrobots: trajectory control of an autonomous tractor using type-2 fuzzy logic controllers," *IEEE/ASME Transactions on Mechatronics*, vol. 20, no. 1, pp. 287–298, 2014.

[33] J. Pérez, V. Milanés, and E. Onieva, "Cascade architecture for lateral control in autonomous vehicles," *IEEE Transactions on Intelligent Transportation Systems*, vol. 12, no. 1, pp. 73–82, 2011.

[34] V. Fors, B. Olofsson, and L. Nielsen, "Formulation and interpretation of optimal braking and steering patterns towards autonomous safety-critical manoeuvres," *Vehicle System Dynamics*, vol. 57, no. 8, pp. 1206–1223, 2019.

[35] C. Ordonez, O. Y. Chuy, E. G. Collins et al., "Rut tracking and steering control for autonomous rut following," in *Proceedings of the 2009 IEEE International Conference on Systems, Man and Cybernetics*, pp. 2775–2781, San Antonio, TX, USA, October 2009.

[36] C. Ordonez, O. Y. Chuy Jr, E. G. Collins Jr, and X. Liu, "Laser-based rut detection and following system for autonomous ground vehicles," *Journal of Field Robotics*, vol. 28, no. 2, pp. 158–179, 2011.

[37] F. Chen, M. Song, X. Ma, and X. Zhu, "Assess the impacts of different autonomous trucks' lateral control modes on asphalt pavement performance," *Transportation Research Part C: Emerging Technologies*, vol. 103, pp. 17–29, 2019.

[38] S. Wang and J. Zhao, "Risk preference and adoption of autonomous vehicles," *Transportation Research Part A: Policy and Practice*, vol. 126, pp. 215–229, 2019.

[39] S. Rajendran, S. K. Spurgeon, G. Tsampardoukas, and R. Hampson, "Estimation of road frictional force and wheel slip for effective antilock braking system (ABS) control," *International Journal of Robust and Nonlinear Control*, vol. 29, no. 3, pp. 736–765, 2019.

[40] Z. Qi, Q. Shi, and H. Zhang, "Tuning of digital PID controllers using particle swarm optimization algorithm for a CAN-based DC motor subject to stochastic delays," *IEEE Transactions on Industrial Electronics*, vol. 67, no. 7, pp. 5637–5646, 2020.

[41] G. Wang, *Study on Completion Evaluation Standards of Key Indicators For Initial Operation of Asphalt Pavement*, Master dissertation, Chang'an University, Xi'an, China, 2013.

[42] Y. Lv, *Research of Chinese Passenger Car Firms' Pricing, Product and Capacity Strategic Behaviors*, Ph.D. thesis, Liaoning University, Shenyang, China, 2012.

[43] C. Xie, *A Study of Passenger Car Buying Behavior and Demand Based on Household Survey Data*, Ph.D. Thesis, Jilin University, Changchun, China, 2014.

[44] X. Liu, Q. Cao, H. Wang, J. Chen, and X. Huang, "Evaluation of vehicle braking performance on wet pavement surface using an integrated tire-vehicle modeling approach," *Transportation Research Record: Journal of the Transportation Research Board*, vol. 2673, no. 3, pp. 295–307, 2019.

[45] International Organization for Standardization, *Mechanical Vibration and Shock-Evaluation of Human Exposure to Whole-Body Vibration-Part 1: General Requirements*, International Organization for Standardization, London, UK, 1997.